Latin American Journal of Energy Research - Lajer
periodicos.ufes.br/lajer

Latin American Journal of Energy Research – Lajer (2024) v. 11, n. 2, p. 81–91
https://doi.org/10.21712/lajer.2024.v11.n2.p81-91

Modeling two-phase flow in converging channels using deformable and fixed methods to describe the interface

Oldrich Joel Romero

Professor in the Graduate Program in Energy, Federal University of Espírito Santo – Ufes, São Mateus campus, ES, Brasil
E-mail: oldrich.romero@ufes.br

Received: 1 December 2024 | Accepted: 17 December 2024 | Published online: 26 December 2024

Abstract: Several methods have been developed in recent years for the solution of free surface flows. These methods can be divided into two main categories: moving grid methods (also known as Lagrangian or interface tracking methods), and fixed grid methods (also known as Eulerian or interface capturing methods). In the first approach the mesh has grid points on the interface and each computational cell contains the same fluid phase. The principal advantages are the simplification of the imposition of boundary conditions on the interface and the high accuracy of the description of the interface configuration and curvature, therefore, this method should be used to solve problems in which capillary forces are important. In the second approach, the boundary of a two-fluid interface is implicitly "captured" solving a scalar equation – pseudo-concentration method (Thompson, 1986) – on the entire stationary grid, i.e. there is a predefined grid that does not move with the interface. The interface may undergo large deformations, and it is relatively straightforward to handle multiple interfaces. However, the high accuracy of the description of the interface configuration is lost. In this paper, the performance of both approaches is compared by analyzing the interface between two Newtonian liquids flowing in two convergent channels that merge into a single channel. The effect of the flow rate of each liquid and viscosity ratio are analyzed. The differential equations that describe the flow are solved by Galerkin/FEM.
Keywords: two-phase flow; moving grid methods; fixed grid methods; Galerkin/FEM.

1 Introduction

In nature and industrial processes, multiphase flows (which include two-phase flow) are the rule rather than an exception. Coating, combustion, boiling heat transfer, rain, material microstructure, oil recovery, are just a few examples. The difficulty in the numerical prediction of multiphase, immiscible flows is the precise location of the interface.

As discussed by Anderson et al. (1998), the interface between two fluids can be represented as a surface of zero thickness endowed with physical properties such as surface tension. Physical quantities, such as density, are discontinuous across the interface thereby rendering the numerical simulation more delicate. Physical processes occurring on the interface are represented by boundary conditions imposed there. This is the classical fluid mechanical approach, which results in a free-boundary problem. In the other approach, the interface is considered diffuse with a non-zero thickness, which is the fundamental assumption of diffuse-interface models, and is (if it refers to approach-singular) based on gradient theories for the interface supported by thermodynamic principles. For details see Anderson et al. (1998), Jacmin (1999) and Pengtao et al. (2004).

In recent years, several methodologies have been developed for addressing this type of problem. Depending on the type of grid used, these methods can be divided into two main categories (Hyman, 1984; Floryan and Rasmussen, 1989), as follows: (i) moving grid methods, also known as Lagrangian or interface tracking methods (Figure 1a); and (ii) fixed grid methods, also known as Eulerian or interface capturing methods (Figure 1b). A combination of these two techniques is considered as hybrid method.

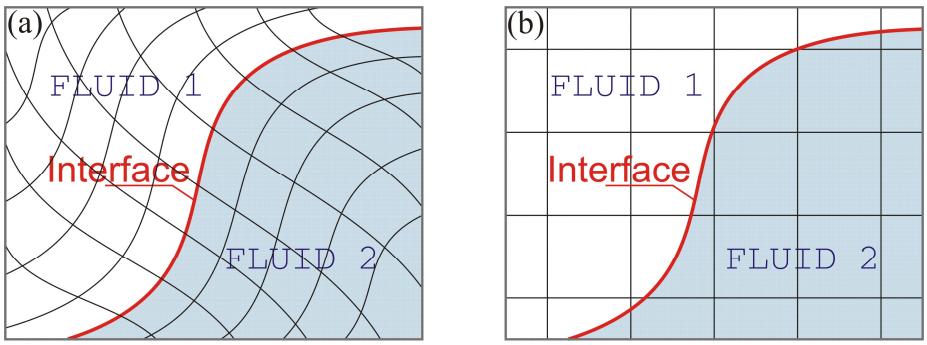

Figure 1. Schematic representation of the interface by (a) Lagrangian and (b) Eulerian methods.

In moving grid methods, the interface is a boundary between two subdomains, the mesh has grid points on the interface, and each computational cell contains the same fluid. The concept is illustrated in Figure 1(a). The principal advantage of this approach is the simplification of the imposition of boundary conditions on the interface, and its more precise localization under small and mild deformations. Inaccuracy associated with "numerical smearing" is ab-sent. The implementation of such techniques is not trivial. It entails a substantial computational overhead, especially in three-dimensional problems. The case of multiple interfaces demands even more care. Changes in topology, as for example breakup, reconnection or coalescence, cannot be handled and significant deformations may cause loss of accuracy. Examples of application of this technique, especially in slot coating process, are in Romero and Carvalho (2008), Romero et al. (2006a), Romero et al. (2006a), Romero et al. (2004).

The second approach, known as fixed grid methods, involves implicitly "capturing" the boundary of a two-fluid interface through the solution of a scalar equation on the entire stationary grid. That is to say, a predefined grid is utilized that remains static with respect to the interface, as illustrated in Figure 1(b), where the fluid travels between different computational cells. The interface may undergo large deformations without, in principle, loss of accuracy, and is relatively straightforward to handle multiple interfaces. This technique is capable of computing geometric properties of highly complicated boundaries without explicitly tracking the interface. It automatically takes care of merging and breaking of the interface. Furthermore, generalizes well to three dimensions. However, modeling the zero-thickness interface is less accurate, and the boundary conditions treatment is more delicate; loss of mass conservation and thick interface thickness are other important drawbacks. An application that combines these two techniques simultaneously in a dual-layer slot coating will be presented in Romero (2025).

In the present paper, both numerical approaches are applied, and their performance is compared in the description of the interface created by two incompressible Newtonian fluids flowing in two branches of planar converging channels, as shown in Figure 2. The techniques selected to describe the interface were elliptic mesh generation (de Santos, 1991), in the context of moving grid methods, and the pseudo-concentration (Thompson, 1986) which belongs to the fixed grid method approach. An investigation is conducted into the effect of the flow rates, fluid viscosities, and numerical parameters on fluid flow behavior.

2 Methodology

2.1 Physical model

The two-dimensional problem with a liquid-liquid interface considered herein is shown schematically in Figure 2. Two planar and symmetrical channels, with different liquids (Liquid 1 and Liquid 2) merge in one forming a liquid-liquid interface.

This geometry, with small angles between dies (i.e. $\theta = 30^o$), is used, for example, in coextrusion process to produce high functional polymers products. An additional application pertains to the domain of emulsion preparation, with particular relevance to chemical enhanced oil recovery.

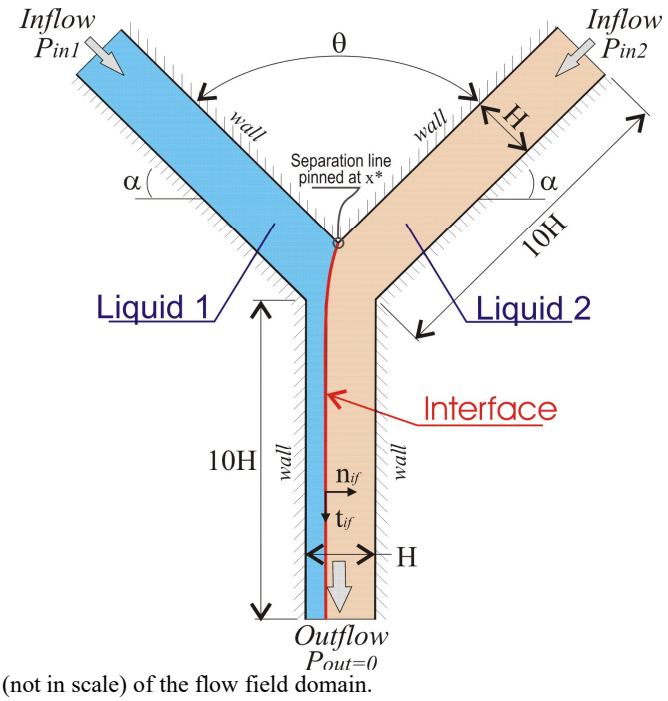

Figure 2. Simplified diagram (not in scale) of the flow field domain.

2.2 Mathematical model

The motion of the inertialess, isothermal, steady-state, viscous fluid is governed by the Navier-Stokes equations, subject to the constraint of divergence-free velocity field applied to each layer separately.

$$\nabla \cdot \mathbf{T}_i = 0, \quad \nabla \cdot \mathbf{v}_i = 0, \tag{1}$$

where $i = 1$ and $i = 2$ denotes liquid 1 and liquid 2 respectively; $\mathbf{T}_i = -p_i\mathbf{I} + \mu_i[\nabla\mathbf{v}_i + (\nabla\mathbf{v}_i)^T]$ is the total stress tensor; $\nabla\boldsymbol{v}$ is the velocity gradient tensor; p is the pressure and $\mathbf{v}_i$ the velocity vector. Gravity effects are neglected. In the classical hydrodynamic approach this formulation results in a free-boundary problem. In the bulk of the fluids, viscosity μ_i is constant in each phase.

Physical information introduced by boundary conditions are the mathematical requirement, necessary to uniquely solve the governing equations of fluid mechanics. According to Figure 2, the boundary conditions are:

- at the two inflow planes, the flow is assumed to be fully developed parallel recti-linear flow with prescribed pressure $P_{in1} = 1$ and different P_{in2} values;
- the no-slip and no-penetration conditions applies to the channels walls;
- at the outflow plane, fully developed flow with pressure prescribed $Pout = 0$ is applied;
- where the interface intersects a solid surface there is a stagnation line (appears as a point in a cross-section of 2D flow) called separation point. This point is considered pinned to the sharp edge formed by the two planes. This treatment of the boundary condition is applied only with the elliptic mesh generation method;
- all along the interface, the forces exerted by pressure and viscous traction must balance. Capillary pressure is negligible, because in this preliminary study liquids are considered miscible. The liquids in contact have a thin layer of interdiffusing components of liquids 1 and 2. Once there is no mass transfer along the interface, the mass balance is represented by the kinematic condition.

Two dimensionless parameters are of particular significance for the purpose of comparing results and will be utilized extensively in the subsequent sections of this study:

- viscosity ratio, $\mu_R = \mu_2 / \mu_1$,
- pressure ratio, $P_R = P_{in} / P_{in}$,

where μ_1 and μ_2 are the constant viscosities of liquids flowing in each plane, P_{in1} and P_{in2} are the imposed pressure at the entrance of each channel.

2.3 Description of the two-phase flow

2.3.1 Moving grid method: elliptic mesh generation

Because of the interface, the flow domain is unknown a priori. For an accurate solution to this kind of problem, the so-called boundary conforming meshes, that deform in response to changes in boundary shape, are particularly well suited. Element boundaries coincide with interfaces (or free surfaces), and accurately tracks the position and shape of the unknown moving boundary.

By mapping the curvilinear coordinates defined on the unknown physical domain $\boldsymbol{\Omega}$ into a known reference domain $\overline{\boldsymbol{\Omega}}$, as indicated in Figure 3, all computation can be performed on rectangular coordinates regardless of the movement of the physical interface.

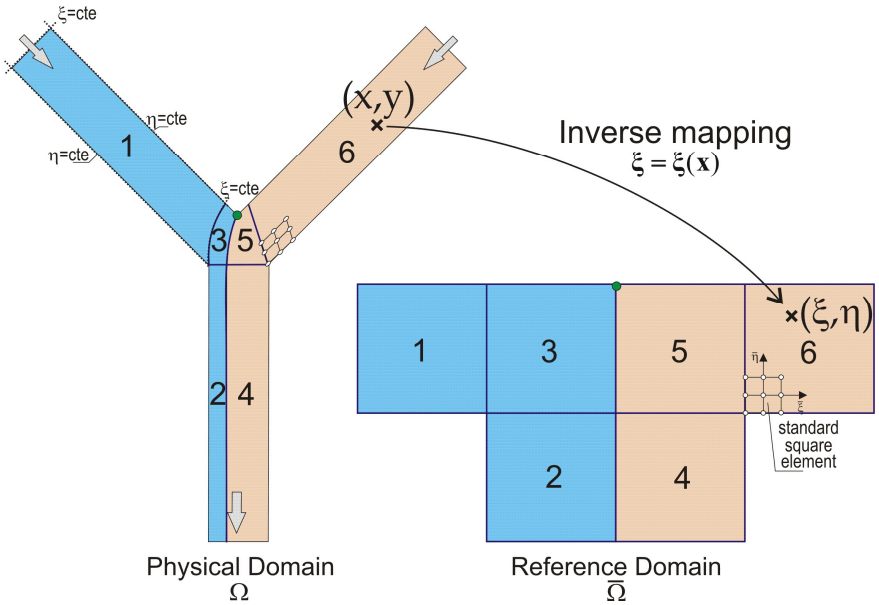

Figure 3. Mapping from a physical domain to a reference domain.

The mapping used here is the one chosen by de Santos (1991) and discussed in more detail by Benjamin (1994). The inverse of the mapping $\boldsymbol{\xi} = \boldsymbol{\xi}(\mathbf{x})$ is governed by a pair of elliptic differential equations. The coordinate potentials ξ and η on the reference domain satisfy

$$\nabla \cdot \left(D_\xi \nabla \xi\right) = 0, \qquad \nabla \cdot \left(D_\eta \nabla \eta\right) = 0\,, \tag{2}$$

D_ξ and D_η are diffusion-like coefficients used to control gradients in coordinate potentials, and thereby the spacing between curves of constant ξ on the one hand and of constant η on the other, that make up the sides of the elements that are employed; they are quadrilateral elements.

Boundary conditions are needed in order to solve the second-order partial differential equations. The solid walls and synthetic inlet and outlet planes are described by functions of the coordinates, and along them stretching functions are used to distribute the termini of the coordinate curves selected to serve as element sides. The liquid-liquid interface requires imposing the kinematic condition. The discrete version of the mapping equations is commonly referred to as mesh generation equations.

2.3.2 Fixed grid method: species concentration equation

The liquid-liquid interface is determined solving a passive scalar equation in the entire domain for a pseudo-concentration c in a stationary flow, advected according to the local velocity (Thompson, 1986)

$$\mathbf{v} \cdot \nabla c = 0 \tag{3}$$

This can be regarded as a conservation equation of color function, which identifies each fluid, and is inspired by the finite volume approach of the volume-of-fluid (VOF) method (Hirt and Nichols, 1981). Because it is a purely convective equation, boundary conditions are only necessary in the two inflow planes,

see Figure 2. Uniform pseudo-concentration was applied to the two entries, $c_{in1} = -1$ for liquid 1, $c_{in2} = +1$ for liquid 2. The crossover region, i.e. where $c = 0$, represents the interface implicitly lo-cated, which is maintained to have some finite thickness by numerical diffusion. The fluid layers were differentiated by their species concentrations and the interfacial region separating the layers was defined as a narrow region between the highest and lowest concentration.

The material properties as they appear in the Navier-Stokes equations can now be determined locally as a function of the material label. Viscosity is constant in each liquid and take on two different values μ_1 or μ_2, depending on the sign of c, through the Heaviside function $H(c)$, if $c < 0$ then $H(c) = 0$, if $c > 0$ then $H(c) = 1$, hence we may write

$$\mu(c) = \mu_1[1 - H(c)] + \mu_2 H(c). \tag{4}$$

Sharp changes in pressure due to large viscosity ratios μ_R (or density ratios when considered) across the front, can present numerical difficulties. To alleviate these problems the smoothed Heaviside function $H_\varepsilon(c)$ is used instead of $H(c)$. The smoothed Heaviside function is defined as

$$H_\varepsilon(c) = \begin{cases} 0 & if \quad c < \varepsilon \\ \frac{1}{2}\left[1 + \frac{c}{\varepsilon} + \frac{1}{\pi} sin\left(\pi \frac{c}{\varepsilon}\right)\right] & if \quad |c| \le \varepsilon \\ 1 & if \quad c > \varepsilon \end{cases} \tag{5}$$

ε is the interface numerical thickness proportional to the finest spatial-mesh size along the flow direction (Δx), a practical rule could be $\Delta x < \varepsilon < 3\Delta x$.

The Navier-Stokes equation, Eq. (1), for each fluid, can be combined into the following single equation valid in the entire domain containing both fluids

$$\nabla \cdot \left[-p\mathbf{I} + \mu(c)[\nabla \mathbf{v} + (\nabla \mathbf{v})^{\mathrm{T}}]\right] = 0, \qquad \nabla \cdot \mathbf{v} = 0. \tag{6}$$

The above equations are used to compute the flow over the whole stationary domain and the interface is advected with the flow. As this study is in its initial stage, the liquids are considered to be miscible, and the interfacial tension is assumed to be negligible.

2.4 Numerical details

In the context of moving grid method, the set of differential equations that describe the conservation of mass and momentum for each liquid, Eq. (1), the mapping between the physical and reference domain, Eq. (2), together with the appropriate boundary conditions, are all solved on the reference domain by the Galerkin / Finite Element Method. Galerkin formulation has proved to be an effective approach for solving elliptic partial differential equations, i.e. Navier-Stokes equations at low Reynolds numbers.

However, the transport equation for the pseudo-concentration, Eq. (3), is hyperbolic and cannot be solved effectively using Galerkin technique because unphysical spurious oscillations pollute the solution. Several stabilized numerical methods have been proposed in the literature to avoid these difficulties: the discontinuous-Galerkin method (Lesaint and Raviart, 1974), the streamline-upwind Petrov-Galerkin – SUPG (Brooks and Hughes, 1982), among others. In this work the SUPG method is selected because it offers more versatility and accuracy. The numerical stabilization is applied by means of the Petrov-Galerkin weighting function ϕ_{PG} which is obtained upwinding the Galerkin weighting function ϕ_G

$$\phi_{PG} = \phi_G + he_i \frac{\boldsymbol{v}}{\|\boldsymbol{v}\|} \cdot \nabla \phi_G, \tag{7}$$

where he_i is the upwinding constant parameter for each liquid, equal to the characteristic size along the flow direction of the smallest element in the mesh.

The position (x, y), velocity (u, v) and pseudo-concentration (c) fields are represented as a linear combination of Lagrangian biquadratic basis functions, and the pressure (p) field as a linear combination of linear discontinuous basis functions.

The set of nonlinear algebraic equations that arises from applying the method of weighted residuals and the representation of the variables in terms of basis functions is solved by Newton's method with

analytical Jacobian, a first order arc-length continuation (Bolstad and Keller, 1986) and a bordering algorithm (Keller, 1977). The tolerance of the L2-norm of the residual vector and the last Newton update for each solution is set to 10^{-6}.

2.5 Obtaining the first solution

To get the very first solution, the two-phase problem is recommended to be simplified considering for example equal viscosities for both liquids $\mu_1 = \mu_2$, and equal pressure in the two inflow planes $P_{in1} = P_{in2}$. Under these conditions both liquids meet forming a perfectly symmetry flow the solution is more straightforward to obtain. The continuity and momentum equations are solved in a fixed geometry, the interface is considered temporarily fixed. The resulting solution is a good enough initial guess for the interface problem. Next steps in the solution process depend on the method employed to describe the interface.

In the moving grid method, a pair of differential elliptic mesh generation locates the mesh points. The free-surface flow problem is solved with high interfacial tension σ_{if} and gradually diminished until $\sigma_{if} = 0$. The number of unknowns are 15,256 and it takes 30 seconds by iteration in a Pentium(R) Core(TM)2 Duo, 2.4 GHz and 4.00 GB RAM computer.

In the fixed grid method, a scalar convective dominated equation captures implicitly the interface. Small values for the upwinding parameters (he_1 and he_2) are selected at the beginning of the process. The number of unknowns is 12,021 and it takes 20 seconds by iteration.

In both cases a continuation technique is applied to proceed to the first solution of the more representative problem. Flow parameters and boundary conditions can be varied step by step always observing the position and form of the liquid-liquid interface.

3 Results and discussions

3.1. Description of the interface by both techniques

The evolution of the interface described by the elliptic mesh method at different input pressures is shown in Figure 4. The changing area where the interface is located becomes highly deformed when the input pressure in channel 2 (Pin_2) is gradually increased, ranging from 1 to 2. The element close to the separation point is especially affected by this deformation.

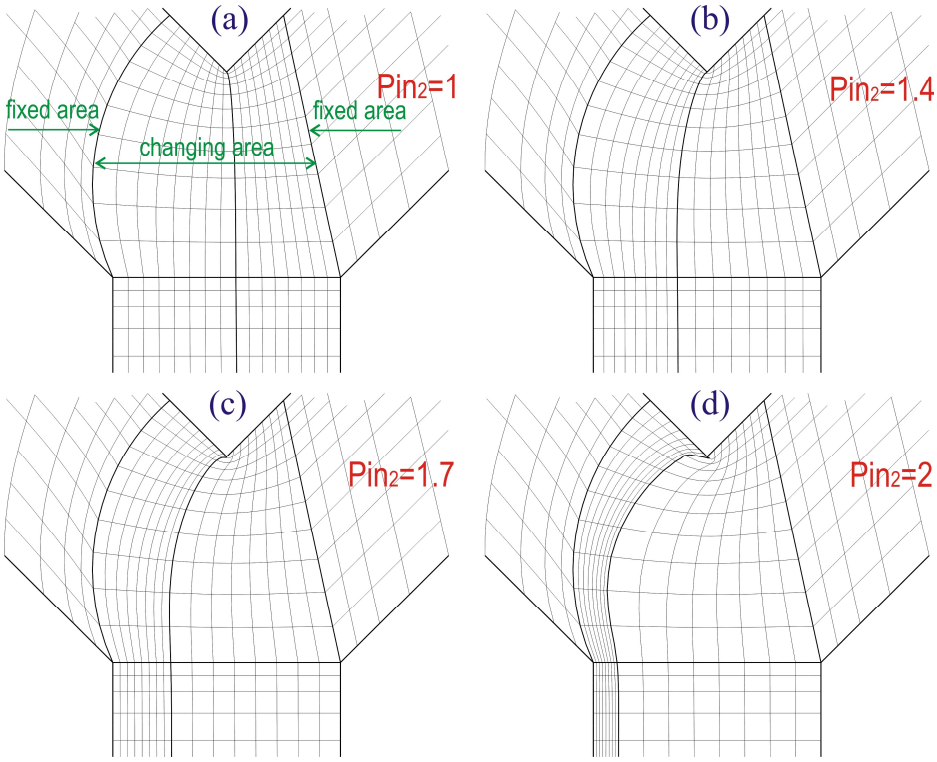

Figure 4 Mesh obtained by the elliptic mesh method at different pressure ratios P_R ($Pin_1 = 1$, different Pin_2).

Figure 5 shows a comparison of the interface obtained by elliptic mesh generation and pseudo-concentration methods. Liquid 1 in the left branch (blue color in the online version), and for liquid 2 right branch (red color in the online version). Streamlines and deformable meshes are also observed. The interface and flow field are very well described by the two methods. The moving grid method is characterized by mesh deformation in accordance with the fluid's movement. This method ensures precise location of the interface at the element boundary, a feature that is absent in the fixed grid method.

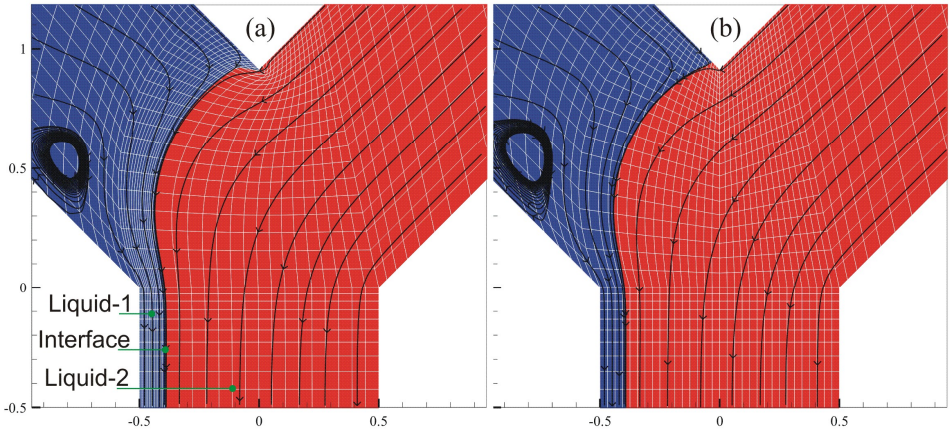

Figure 5. Comparison of the two approaches in the description of the interface, (a) elliptic mesh method and (b) pseudo-concentration method ($he_1 = he_2 = 0.3$). In both cases $\mu_R = 1.5$ ($\mu_1 = 1, \mu_2 = 1.5$) and $P_R = 2$ ($Pin_1 = 1, Pin_2 = 2$).

Comparisons of velocity profiles at the outflow plane for different viscosity ratio and constant pressure ratio P_R is presented in Figure 6(a). The bulges at high viscosity ratio are characteristic of multilayer flow fluid. The figure also shows the very well response of both techniques in the description of the velocity profile at $\mu_R = 1.5$ and $P_R = 2$.

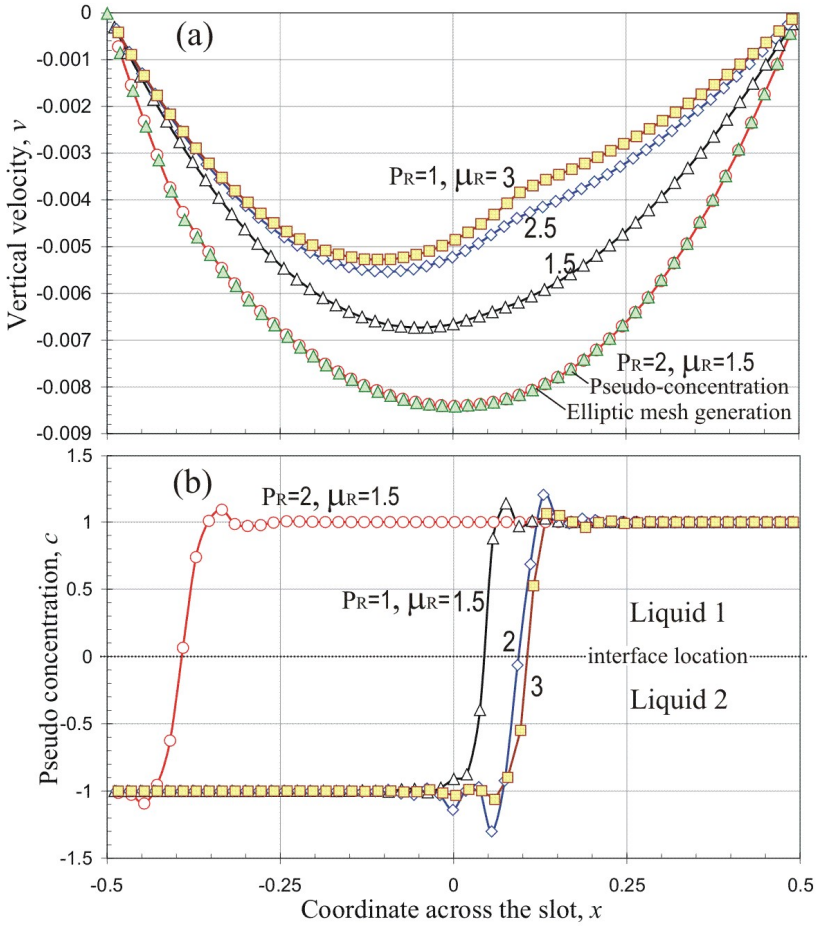

Figure 6. (a) vertical velocity and (b) pseudo-concentration variable profiles plotted at the outflow plane at different viscosity ratios. Upwinding parameters used are $he_1 = he_2 = 0.1$ (at $P_R = 1$) and $he_1 = he_2 = 0.3$ (at $P_R = 2$).

In Figure 6(b) the numerical pseudo-concentration variable is plotted in the outlet plane at different viscosity ratio μ_R. As expected, the concentration takes values of $c = -1$ in the liquid 1, $c = +1$ in the liquid 2, and $c = 0$ at the interface.

Overshoots and undershoots are presented close to the interface since a discontinuity is transported. As expected, at the same viscosity ratio, when pressure in channel 2 is higher, the interface moves to the left side. Compare interface position at $P_R = 2$ and at $P_R = 1$. Also in the figure, at same pressure ratio, the interface moves to the right side of the channel when viscosity ratio increases.

3.2 Performance of the pseudo-concentration method

The evolution of the concentration flow flied c at different pressure ratio P_R and at constant viscosity ratio $\mu_R = 1.5$, is illustrated in Figure 7.

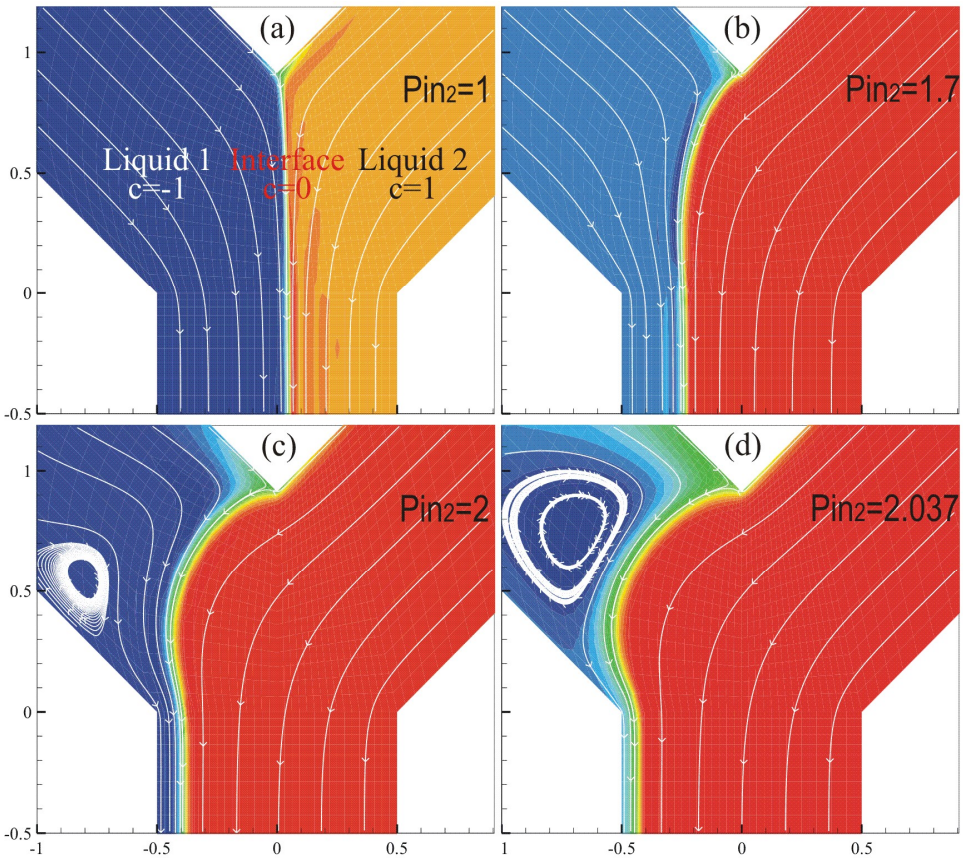

Figure 7. Fluid flow by the pseudo-concentration method at different pressure ratio P_R and constant viscosity ratio $\mu_R = 1.5$. Upwinding parameters used in (a) and (b) are $he_1 = he_2 = 0.1$, in (c) $he_1 = he_2 = 0.3$, and in (d) $he_1 = 0.7$ and $he_1 = 0.5$.

The pressure P_{in2} in the right channel is increased gradually from 1 to 2.037 (slightly higher than 2), but only four representative fields with streamlines are presented. Therefore, the flow in the right channel becomes stronger until almost close the flow in the left branch. An accentuated curvature of the interface invades the channel 1 and a small recirculation appear at $P_{in2} = 1.95$ (not plotted) growing monotonically with the pressure ratio, until reaching the maximal pressure ratio $P_R = 2.037$ at which it is possible to obtain a solution. Close to the critical condition, or turning point, small changes in the input conditions reveal an accentuate increase in the curvature of the interface and recirculation size. Because the momentum equations become convected dominating the pressure ratio increase, the upwinding parameters have to be modified in order to obtain converged solutions, the values used under each condition are shown in the figure caption.

After $P_{in} = 2.037$ no more converged solutions could be reached, even with higher upwinding parameters, so we called this value the critical point. In other numerical experiments a solution was obtained with a very small value after the critical point showing that the strong liquid flow (right branch) invades completely the left branch. A strong numerical diffusion toward the weak flow side is observed close to the separation point and increasing all along the interface when conditions are close to the critical condition.

The results show that the separation point is almost always pinned to the sharp edge of the center block, so the pinned condition prescribed in the elliptic mesh method is reasonable.

It is known that a drawback of fixed-grid methods is a loss of mass conservation. To determine where the numerical diffusion is present, the equation is post-processed and the results are presented in Figure 8. The equation is not satisfied, or is different from zero, close to the interface. Loss of mass is more accentuated when one liquid flow becomes stronger, in this case the liquid flowing in the right channel.

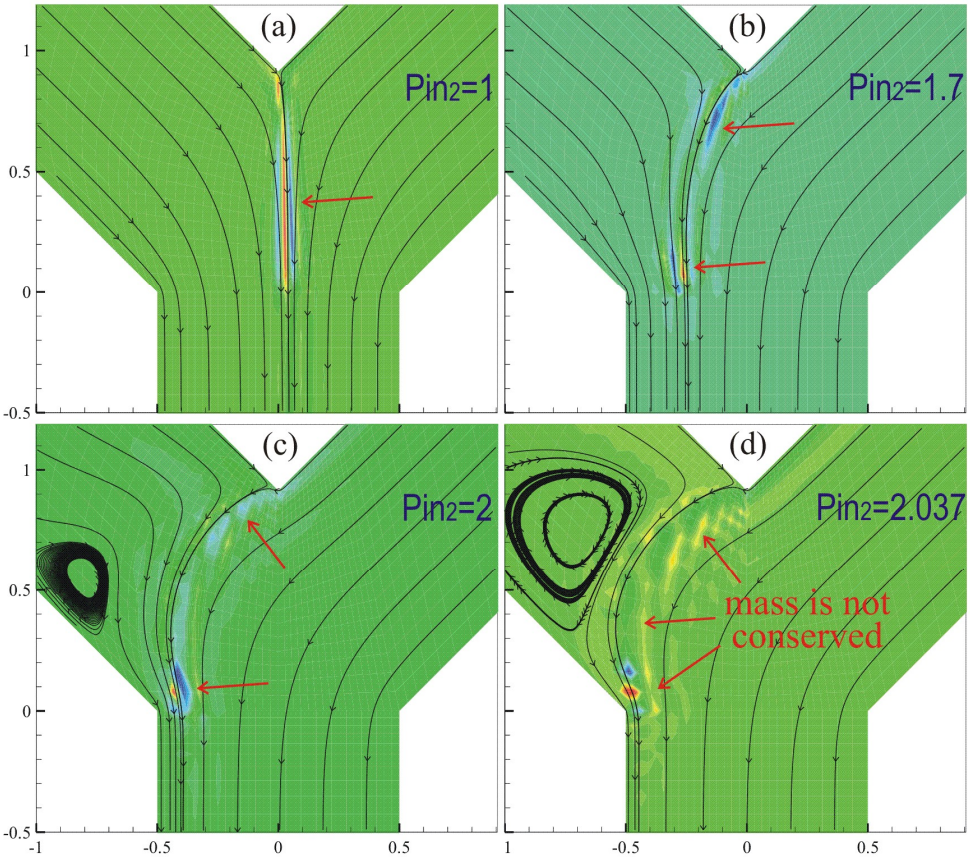

Figure 8. Loss of mass (numerical diffusion) in the flow domain at conditions described in caption of Figure 7.

3.3 Influence of the smearing parameter

The viscosity field $\mu(c)$, given by Eq. (4), depends directly on the smoothed Heavisade function, Eq. (5), and the degree of smoothness is controlled by the interface numerical thickness ε. Three – small, middle and high –values of this parameter are used and its influence in the viscosity field is presented in Figure 9. The viscosity ratio and the pressure ratio are $\mu_R = 1.5$ and $P_R = 2$, respectively.

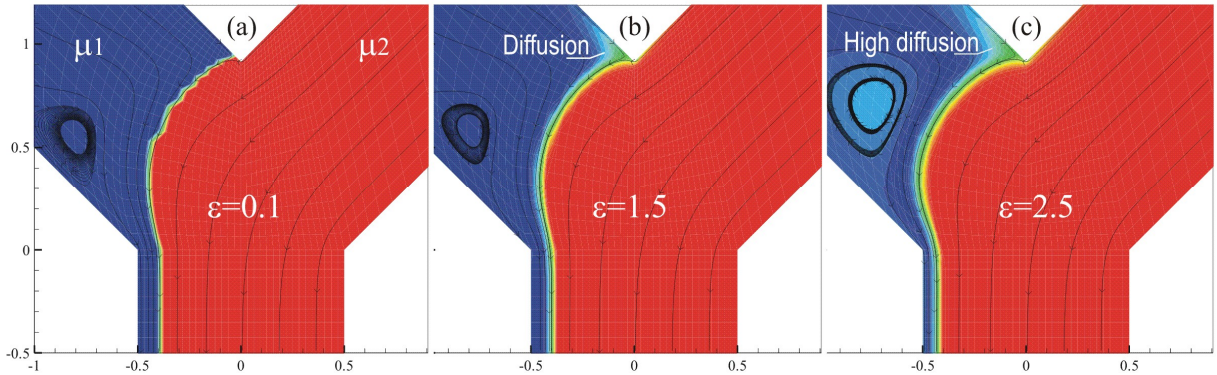

Figure 9. Influence of the smearing parameter ε in the viscosity field. Pressure ratio $P_R = 2$, viscosity ratio $\mu_R = 1.5$ and upwinding parameters $he_1 = he_2 = 0.3$, respectively.

The higher the ε parameter is, the higher the thickness of the interface, and the higher the numerical diffusion is. And, because the total stress tensor in the momentum equation for the two fluid flow, Eq. (6),

is affected by the viscosity, higher changes in ε alters the flow field, as shown in the figure. The recirculation becomes bigger, and the center of the recirculation moves towards the center of the feed slot. This happens because the normal viscous stress balance on the interface is modified, making the curvature of the interface more pronounced and displacing it towards the weak fluid flow when a critical value is achieved.

4 Final remarks

The liquid-liquid interface behavior was represented by two different numerical techniques, moving grid method and fixed grid method, at different viscosity and pressure ratios.

In the elliptic mesh generation method, although the computational implementation of the two partial differential equations for the unknown mesh positions, presents an additional difficulty, a better definition of the interface is reached, because it is located on the element side and deforms following the fluid motion. Additionally, problems such as a loss of mass and an adequate choice of the smearing parameter are avoided.

The second technique is based on the solution of a scalar equation, relatively easier to implement but presents some drawbacks: mesh will be fine enough to capture details of the interface, mass in not conserved, and is mandatory for an adequate choice of a non-constant smearing parameter to control the degree of smoothness. The last characteristic is highly dependent on the experience of the user. An inappropriate value could make it impossible to obtain a converged solution or create a high numerical diffusion.

Acknowledgements

Thanks to the Foundation for Research and Innovation of Espírito Santo (Fapes – *Fundação de Amparo à Pesquisa e Inovação do Espírito Santo*) for their financial support through the Capalaba Researcher Scholarship TO 356/2022.

References

Anderson, DM, McFadden, GB and Wheeler, AA (1998) 'Diffuse-Interface Methods in Fluid Mechanics', *Annu. Rev. Fluid Mech*., v. 30, p. 139-165

Benjamin, DF (1994) *Roll Coating Flows and Multiple Rolls Systems*, Doctoral thesis, University of Minnesota, MN, USA.

Bolstad, JH and Keller, HB (1985) 'A multigrid continuation method for elliptic problems whit folds', *SIAM Journal of Science Stat. Comput.,* v. 7, p. 1081-1104.

De Santos, JM (1991) *Two-phase Cocurrent Downflow through Constricted Passages*, Doctoral thesis, University of Minnesota, MN, USA.

Floryan, JM and Rasmussen, H (1984) 'Numerical Methods for Viscous Flows with Moving Interfaces' *Appl. Mech. Rev.*, v. 42, n. 12, p. 323-341.

Hirt, CW and Nichols, BD (1981) '*Volume of Fluid (VOF) Method for the Dynamics of free Boundaries*', *J. Comput. Phys.*, v. 39, p. 201-225.

Hyman, JM (1984) 'Numerical Methods for Tracking Interfaces', *Physica 12D*, p. 396-407.

Jacmin, D (1999) 'Calculation of two-phase Navier-Stokes Flows Using Phase-Field Model-ing', *J. Comput. Phys*., v. 155, p. 96-127.

Keller, HB (1977) 'Numerical solution of bifurcations and nonlinear eigenvalue problems' in ed. PH Rabinowitz, *Applications of Bifurcation Theory*. New York: Academic Press, p. 45-52.

Lesaint, P and Raviart PA (1974) 'On a finite element method for solving the neutron transport equation', in ed.C de Boor, *Mathematical aspects of finite elements in partial differential equations*. New York: Academic Press, p. 89-123.

Pengtao, Y, Feng, JJ, Chun, L and Shen, J (2004) 'A Diffuse-Interface Method for Simulating Two-Phase Flows of Complex Fluids', *J. Fluid Mech.*, v. 515, p. 293-317.

Romero, OJ (2025) ‘Hybrid approach simulation for two-layer slot coating’, *in preparation*.

Romero, OJ, Carvalho, MS (2008) ‘Response of slot coating flows to periodic disturbances’, *Chemical Engineering Science*, v. 63, p. 2161-2173.

Romero, OJ, Scriven, LE and Carvalho, MS (2006) ‘Effect of curvature of coating die edges on the pinning of contact line’, *AIChE Journal*, v. 52, p. 447-455.

Romero, OJ, Scriven, LE and Carvalho, MS (2006) ‘Slot coating of mildly viscoelastic liquids’, *Journal of Non-Newtonian Fluid Mechanics*, v. 138, p. 63-75.

Romero, OJ, Suszynsky, W, Scriven, LE and Carvalho, MS (2004) ‘Low-flow limit in slot coating of diluted solutions of high molecular weight polymer’, *Journal of Non-Newtonian Fluid Mechanics*, v. 118, p. 137-156.